

MODELLING FOR MECHANICAL ELEMENTS OF T-SHAPED CROSS-SECTIONAL BEAMS WITH STRAIGHT HAUNCHES: PART II

OMAR SIERRA-ANDRADE¹, ARNULFO LUÉVANOS-ROJAS^{1,*}
AND BLANCA ESTELA MONTANO-PÉREZ²

¹Facultad de Contaduría y Administración
Universidad Autónoma de Coahuila, Unidad Torreón
Blvd. Revolución 151 Ote. CP 27000, Torreón, Coahuila, México
omarsierraandrade@uadec.edu.mx; *Corresponding author: arnulfoluevanos@uadec.edu.mx

²Facultad de Contaduría y Administración
Universidad Autónoma de Coahuila, Unidad Norte
Blvd. Harlod R. Pape K 4.5. CP 25710, Monclova, Coahuila, México
blancamontanoperez@uadec.edu.mx

Received May 2023; revised September 2023

ABSTRACT. *The first part of this paper shows a model for T-shaped cross-sectional beams with straight haunches under a uniformly distributed load that considers shear and bending deformations to obtain the fixed-end moments, carry-over and stiffness factors. Now, this paper shows a model for the T-shaped beams with straight haunches under a concentrated load localized anywhere of the beam that takes account of bending and shear deformations to obtain the fixed-end moments, which is the main part of this investigation. The methodology used is the same procedure applied in Part I. The traditional model considers only the bending deformations and the shear deformations are neglected, and some authors consider bending and shear deformations for some proportions that are shown in tables. A numerical example has been developed to observe the application of the proposed model, and a comparison among the proposed approach that considers bending and shear deformations against the traditional model that considers bending deformations only is presented in the tables and graphics. A significant advantage is that the fixed-end moments can be obtained for any T-shaped beams with straight haunches using the model proposed in this paper.*

Keywords: T-shaped beams, Fixed-end moments factors, Carry-over factors, Stiffness factors, Concentrated load, Bending and shear deformations

1. Introduction. The main concern of structural engineering is to propose suitable methods that are reliable to satisfactorily modeling non-prismatic cross-sectional members, in such a way that is having certainty in the determination of the mechanical elements, such as deformations and displacements that allow this type of structural members to be properly designed.

The reinforced concrete non-prismatic beams have the following advantages with respect to prismatic beams: 1) Substantially increase lateral stiffness; 2) Promote the more efficient use of concrete and longitudinal reinforcement steel; 3) Reduce the weight of the building; 4) Facilitate the placement of electrical, air conditioning and sanitary installations in the building.

Between the years of 1950 to 1960 several design aids are developed, such as those presented by Guldan [1], and the most popular tables published by the PCA (Portland Cement Association) in 1958 “Handbook” [2].

The most relevant documents dealing the topic of structural members with non-prismatic cross section are discussed in Part I [3-26].

The bibliographic review shows that the closest studies for the T-shaped beams with straight haunches are the tables provided the fixed-end moments, carry-over and stiffness factors for beams of sections in shape of “I” and “T” [7]. These tables for the T-shaped beams consider the flange width “ b_f ” is equal to the web thickness “ b_w ” more 16 times flange thickness “ t_f ”, the relationship between the beam length and the effective depth is equal to 10, the relationship between the flange thickness “ t_f ” and the effective depth is equal to 1/4, the relationship between the web thickness “ b_w ” and the effective depth is equal to 3/4, and the height of the straight haunches is the same in the two ends. Therefore, there are no papers on the subject with the level of current knowledge that provide a way to obtain the fixed-end moments, carry-over and stiffness factors for T-shaped beams with straight haunches for the general case.

This paper shows a mathematical model for T-shaped cross-sectional beams with straight haunches under a concentrated load localized anywhere of the beam considering the bending and shear deformations to find the fixed-end moments. The methodology used is the same procedure applied in Part I. The traditional model only considers the bending deformations, and other authors consider bending and shear deformations for proportions restricted that are shown in tables. A numerical example has been developed to observe the application of the proposed model, and a comparison between the proposed approaches that considers bending and shear deformations against the traditional model that considers bending deformations only are presented in the tables and graphics to observe differences.

The paper is organized as follows. Section 2 shows the formulation of the mathematical model for the equations of fixed-end moments factors. Section 3 describes the application of the proposed model. Section 4 is dedicated to the results through the comparison of the two models, the proposed model (PM), and the traditional model (TM). Section 5 presents the conclusions.

2. Formulation of the Mathematical Model. Figure 1 shows in detail the asymmetric T-shaped beam under a concentrated load where the flange width “ b_f ”, flange thickness “ t_f ”, web thickness “ b_w ” are constant, k is the location of load, GC is center of gravity of the cross section, L_1 and L_2 are the lengths of the haunches, and the web height “ d_x ” that varies with the linear shape at the ends, and the beam in the center has a constant section.

The geometrical properties of the cross section of the T-shaped beam are shown in Equations (1) to (12) of Part I.

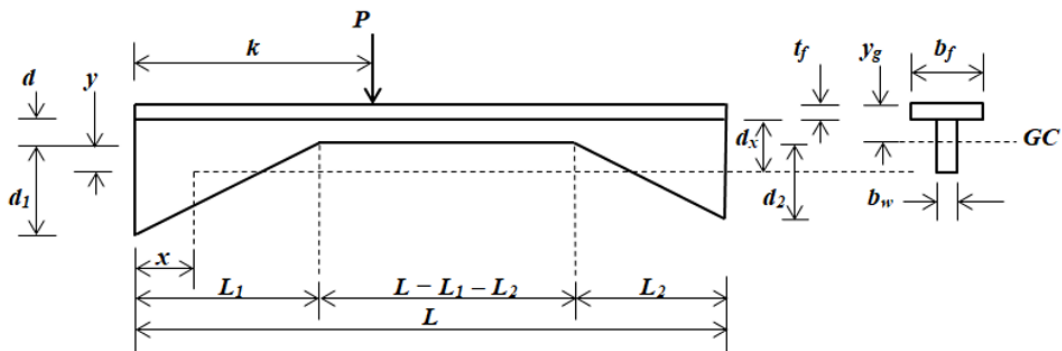


FIGURE 1. T-shaped beam with straight haunches under a concentrated load

Figure 2(a) shows a beam “AB” under a concentrated load located on anywhere of the beam and fixed at its ends for three different cases (Case 1: The load P is located from $0 \leq x \leq L_1$, Case 2: The load P is localized from $L_1 \leq x \leq L - L_2$, Case 3: The load P is located of $L - L_2 \leq x \leq L$) is obtained by the principle of superposition (sum of the individual rotations in each support “A” and “B”). The moments according to the sign are considered: counterclockwise is positive, and clockwise is negative. In Figure 2(b) for all three cases is presented the same simply supported beam at its ends under the load applied to obtaining the rotations “ β_{A1} ” and “ β_{B1} ” for case 1, “ β_{A2} ” and “ β_{B2} ” for the case 2, “ β_{A3} ” and “ β_{B3} ” for case 3. In Figure 2(c) for all three cases is shown the moment “ M_{AB} ” applied in the support “A” that generates the rotations “ β_{A12} ” and “ β_{B12} ” for case 1, “ β_{A22} ” and “ β_{B22} ” for the case 2, “ β_{A32} ” and “ β_{B32} ” for case 3. In Figure 2(d) for all three cases is presented the moment “ M_{BA} ” applied in the support “B” that generates the rotations “ β_{A13} ” and “ β_{B13} ” for case 1, “ β_{A23} ” and “ β_{B23} ” for the case 2, “ β_{A33} ” and “ β_{B33} ” for case 3 [27-32].

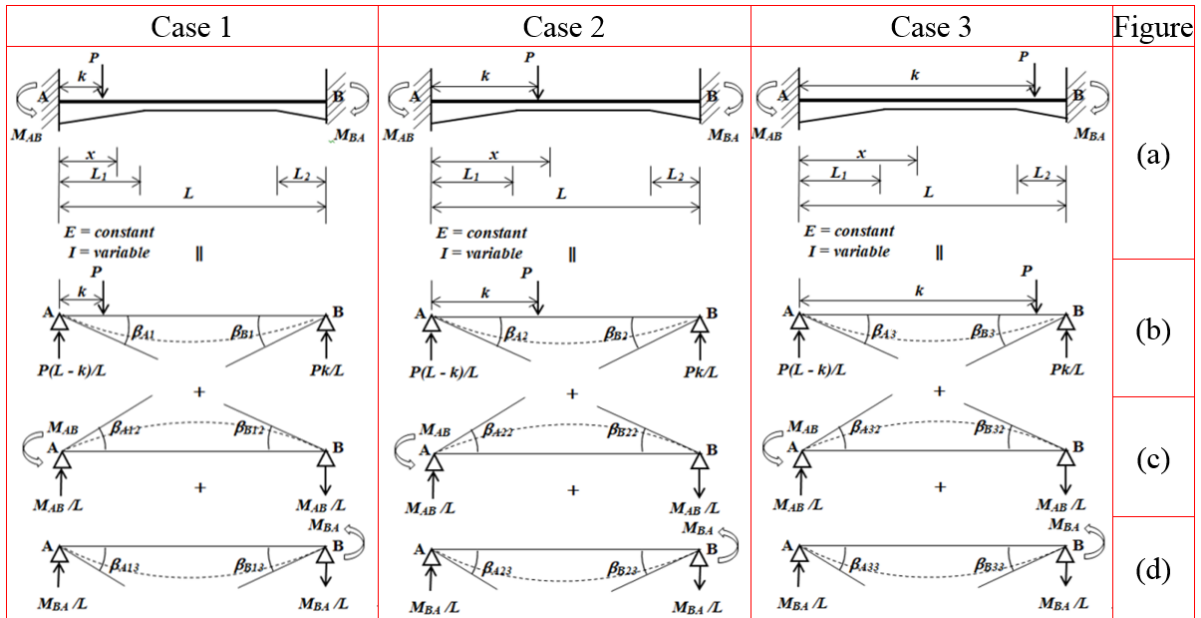


FIGURE 2. T-shaped beam with fixed supports

Now, by the principle of superposition and using the beam compatibility equations for the rotations in each support obtain the following equations:

To $0 \leq x \leq L_1$:

$$\beta_{A1} - \beta_{A12} + \beta_{A13} = 0 \tag{1}$$

$$\beta_{B1} - \beta_{B12} + \beta_{B13} = 0 \tag{2}$$

To $L_1 \leq x \leq L - L_2$:

$$\beta_{A2} - \beta_{A22} + \beta_{A23} = 0 \tag{3}$$

$$\beta_{B2} - \beta_{B22} + \beta_{B23} = 0 \tag{4}$$

To $L - L_2 \leq x \leq L$:

$$\beta_{A3} - \beta_{A32} + \beta_{A33} = 0 \tag{5}$$

$$\beta_{B3} - \beta_{B32} + \beta_{B33} = 0 \tag{6}$$

Figure 2(a) for the three cases is analyzed to obtain the rotations (β_{A1} and β_{B1} , β_{A2} and β_{B2} , β_{A3} and β_{B3}) and the bending and shear deformations are taken into account due to the loads applied on beam.

The rotations for non-prismatic members are obtained by Equations (15) and (16) of Part I.

The shear forces and moments located in anywhere on the beam for the three cases according to Figure 2(b) are

To $0 \leq x \leq k$:

$$V_x = \frac{P(L-k)}{L} \quad (7)$$

$$M_x = \frac{P(L-k)x}{L} \quad (8)$$

To $k \leq x \leq L$:

$$V_x = \frac{Pk}{L} \quad (9)$$

$$M_x = \frac{Pk(L-x)}{L} \quad (10)$$

Substituting Equations (7) to (10) into Equations (15) and (16) of Part I, the rotations (β_{A1} and β_{B1} , β_{A2} and β_{B2} , β_{A3} and β_{B3}) are obtained as follows:

To $0 \leq x \leq L_1$:

$$\begin{aligned} \beta_{A1} = & -\frac{P}{GL^2} \left[\int_0^k \frac{(L-k)}{A_{sx1}} dx - \int_k^{L_1} \frac{k}{A_{sx1}} dx - \int_{L_1}^{L-L_2} \frac{k}{A_{sx2}} dx - \int_{L-L_2}^L \frac{k}{A_{sx3}} dx \right] \\ & + \frac{P}{EL^2} \left[\int_0^k \frac{(L-k)(L-x)x}{I_{x1}} dx + \int_k^{L_1} \frac{k(L-x)^2}{I_{x1}} dx + \int_{L_1}^{L-L_2} \frac{k(L-x)^2}{I_{x2}} dx \right. \\ & \left. + \int_{L-L_2}^L \frac{k(L-x)^2}{I_{x3}} dx \right] \end{aligned} \quad (11)$$

$$\begin{aligned} \beta_{B1} = & \frac{P}{GL^2} \left[\int_0^k \frac{(L-k)}{A_{sx1}} dx - \int_k^{L_1} \frac{k}{A_{sx1}} dx - \int_{L_1}^{L-L_2} \frac{k}{A_{sx2}} dx - \int_{L-L_2}^L \frac{k}{A_{sx3}} dx \right] \\ & + \frac{P}{EL^2} \left[\int_0^k \frac{(L-k)x^2}{I_{x1}} dx + \int_k^{L_1} \frac{k(L-x)x}{I_{x1}} dx + \int_{L_1}^{L-L_2} \frac{k(L-x)x}{I_{x2}} dx \right. \\ & \left. + \int_{L-L_2}^L \frac{k(L-x)x}{I_{x3}} dx \right] \end{aligned} \quad (12)$$

To $L_1 \leq x \leq L-L_2$:

$$\begin{aligned} \beta_{A2} = & -\frac{P}{GL^2} \left[\int_0^{L_1} \frac{(L-k)}{A_{sx1}} dx + \int_{L_1}^k \frac{(L-k)}{A_{sx2}} dx - \int_k^{L-L_2} \frac{k}{A_{sx2}} dx - \int_{L-L_2}^L \frac{k}{A_{sx3}} dx \right] \\ & + \frac{P}{EL^2} \left[\int_0^{L_1} \frac{(L-k)(L-x)x}{I_{x1}} dx + \int_{L_1}^k \frac{(L-k)(L-x)x}{I_{x2}} dx \right. \\ & \left. + \int_k^{L-L_2} \frac{k(L-x)^2}{I_{x2}} dx + \int_{L-L_2}^L \frac{k(L-x)^2}{I_{x3}} dx \right] \end{aligned} \quad (13)$$

$$\begin{aligned} \beta_{B2} = & \frac{P}{GL^2} \left[\int_0^{L_1} \frac{(L-k)}{A_{sx1}} dx + \int_{L_1}^k \frac{(L-k)}{A_{sx2}} dx - \int_k^{L-L_2} \frac{k}{A_{sx2}} dx - \int_{L-L_2}^L \frac{k}{A_{sx3}} dx \right] \\ & + \frac{P}{EL^2} \left[\int_0^{L_1} \frac{(L-k)x^2}{I_{x1}} dx + \int_{L_1}^k \frac{(L-k)x^2}{I_{x2}} dx + \int_k^{L-L_2} \frac{k(L-x)x}{I_{x2}} dx \right] \end{aligned}$$

$$+ \int_{L-L_2}^L \frac{k(L-x)x}{I_{x3}} dx \Big] \quad (14)$$

To $L - L_2 \leq x \leq L$:

$$\begin{aligned} \beta_{A3} = & -\frac{P}{GL^2} \left[\int_0^{L_1} \frac{(L-k)}{A_{sx1}} dx + \int_{L_1}^{L-L_2} \frac{(L-k)}{A_{sx2}} dx + \int_{L-L_2}^k \frac{(L-k)}{A_{sx3}} dx - \int_k^L \frac{k}{A_{sx3}} dx \right] \\ & + \frac{P}{EL^2} \left[\int_0^{L_1} \frac{(L-k)(L-x)x}{I_{x1}} dx + \int_{L_1}^{L-L_2} \frac{(L-k)(L-x)x}{I_{x2}} dx \right. \\ & \left. + \int_{L-L_2}^k \frac{(L-k)(L-x)x}{I_{x3}} dx + \int_k^L \frac{k(L-x)^2}{I_{x3}} dx \right] \end{aligned} \quad (15)$$

$$\begin{aligned} \beta_{B3} = & \frac{P}{GL^2} \left[\int_0^{L_1} \frac{(L-k)}{A_{sx1}} dx + \int_{L_1}^{L-L_2} \frac{(L-k)}{A_{sx2}} dx + \int_{L-L_2}^k \frac{(L-k)}{A_{sx3}} dx - \int_k^L \frac{k}{A_{sx3}} dx \right] \\ & + \frac{P}{EL^2} \left[\int_0^{L_1} \frac{(L-k)x^2}{I_{x1}} dx + \int_{L_1}^{L-L_2} \frac{(L-k)x^2}{I_{x2}} dx + \int_{L-L_2}^k \frac{(L-k)x^2}{I_{x3}} dx \right. \\ & \left. + \int_k^L \frac{k(L-x)x}{I_{x3}} dx \right] \end{aligned} \quad (16)$$

The rotations (β_{A12} and β_{B12} , β_{A22} and β_{B22} , β_{A32} and β_{B32}) on the beam according to Figure 2(c) are

$$\beta_{A12} = \beta_{A22} = \beta_{A32} = \beta_{A2} \text{ (Part I)} \quad (17)$$

$$\beta_{B12} = \beta_{B22} = \beta_{B32} = \beta_{B2} \text{ (Part I)} \quad (18)$$

The rotations (β_{A13} and β_{B13} , β_{A23} and β_{B23} , β_{A33} and β_{B33}) on the beam according to Figure 2(d) are:

$$\beta_{A13} = \beta_{A23} = \beta_{A33} = \beta_{A3} \text{ (Part I)} \quad (19)$$

$$\beta_{B13} = \beta_{B23} = \beta_{B33} = \beta_{B3} \text{ (Part I)} \quad (20)$$

Now, analyze the three cases individually for corresponding intervals.

Case 1: Equation (11), and Equations (23) and (27) of Part I that correspond to support ‘‘A’’ are substituted into Equation (1) to obtain the moment ‘‘ M_{AB} ’’, and Equation (12), and Equations (24) and (28) of Part I that correspond to support ‘‘B’’ are substituted into Equation (2) to obtain the moment ‘‘ M_{BA} ’’ for the load ‘‘ P ’’ located in the interval $0 \leq x \leq L_1$. Subsequently, the generated equations are solved to obtain the values of ‘‘ M_{AB} ’’ and ‘‘ M_{BA} ’’.

Case 2: Equation (13), and Equations (23) and (27) of Part I that correspond to support ‘‘A’’ are substituted into Equation (3) to obtain the moment ‘‘ M_{AB} ’’, and Equation (14), and Equations (24) and (28) of Part I that correspond to support ‘‘B’’ are substituted into Equation (4) to obtain the moment ‘‘ M_{BA} ’’ for the load ‘‘ P ’’ located in the interval $L_1 \leq x \leq L - L_2$. Subsequently, the generated equations are solved to obtain the values of ‘‘ M_{AB} ’’ and ‘‘ M_{BA} ’’.

Case 3: Equation (15), and Equations (23) and (27) of Part I that correspond to support ‘‘A’’ are substituted into Equation (5) to obtain the moment ‘‘ M_{AB} ’’, and Equation (16), and Equations (24) and (28) of Part I that correspond to support ‘‘B’’ are substituted into Equation (6) to obtain the moment ‘‘ M_{BA} ’’ for the load ‘‘ P ’’ located in the interval $L - L_2 \leq x \leq L$. Subsequently, the generated equations are solved to obtain the values of ‘‘ M_{AB} ’’ and ‘‘ M_{BA} ’’.

The equations of the moments for the three cases are presented as follows:

$$M_{AB} = \frac{PL}{m_{AB}} \quad (21)$$

$$M_{BA} = \frac{PL}{m_{BA}} \quad (22)$$

where m_{AB} and m_{BA} are the fixed-end moment factors.

The equations for fixed-end moments “ M_{AB} ” and “ M_{BA} ” are shown in Appendix.

3. Numerical Example of the Proposed Model. Figure 3 illustrates a three-span continuous highway bridge for a reinforced concrete T-shaped beam with straight haunches. The first and third beams (A-B and C-D) have a length of 12.00 m, and have two asymmetrical straight haunches. The second beam (B-C) has a length of 15.00 m, and has two straight haunches, and the haunches are perfectly symmetrical. Figure 4 shows the critical position of the live loads for each stretch of the highway bridge, taking account of the live loads that provide the specifications for the design of bridges [33]. Constant data over all the cross section are $\nu = 0.20$ for concrete, $b_f = 1.50$ m, $t_f = 0.30$ m, $b_w = 0.50$ m. For obtaining the final moments, the proposed model developed through matrix methods is used.

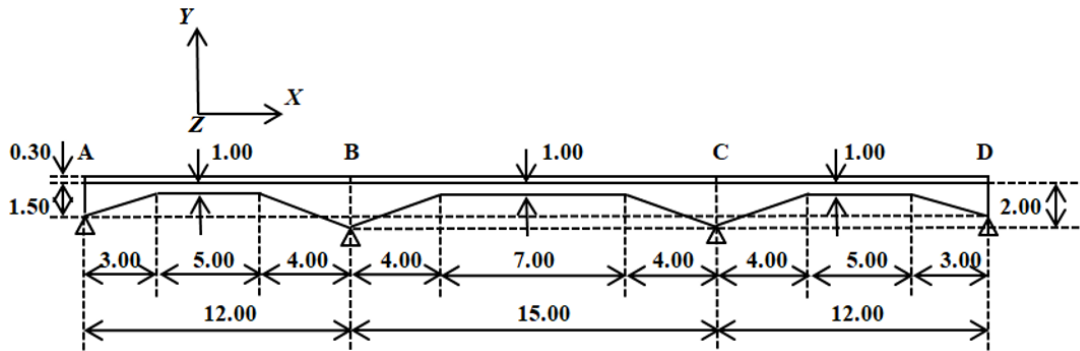
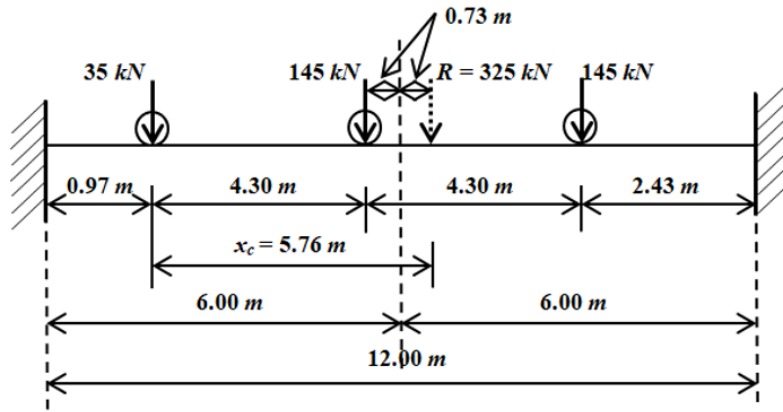


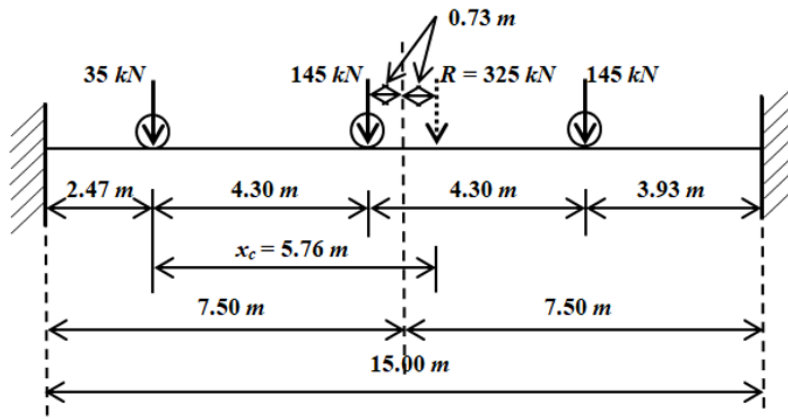
FIGURE 3. Non-prismatic reinforced concrete T-shaped beam

For the beam A-B: $L_1 = 3.00$ m; $L_2 = 4.00$ m; $d = 1.00$ m; $d_1 = 0.50$ m; $d_2 = 1.00$ m; $L = 12.00$ m. To the load $P = 35$ kN, $k = 0.97$ m, and is localized of $0 \leq x \leq L_1$, the fixed-end moments are $M_{AB1} = 29.4629$ kN-m and $M_{BA1} = 3.5294$ kN-m. To the load $P = 145$ kN, $k = 5.27$ m, and is found of $L_1 \leq x \leq L - L_2$, the fixed-end moments are $M_{AB2} = 168.8641$ kN-m and $M_{BA2} = 277.9787$ kN-m. To the load $P = 145$ kN, $k = 9.57$ m, and is located of $L - L_2 \leq x \leq L$, the fixed-end moments are $M_{AB3} = 41.6909$ kN-m and $M_{BA3} = 275.4334$ kN-m. The total fixed-end moments are $M_{ABT} = 240.0179$ kN-m and $M_{BAT} = 556.9415$ kN-m. The carry-over factors by Part I of this paper are obtained: $C_{AB} = 0.6968$ and $C_{BA} = 0.5348$. The stiffness factors by Part I of this paper are obtained: $k_{AB} = 6.2319$ and $k_{BA} = 8.1197$. The absolute stiffnesses are $K_{AB} = 6.2319EI/L$ and $K_{BA} = 8.1197EI/L$.

For the beam B-C: $L_1 = 4.00$ m; $L_2 = 4.00$ m; $d = 1.00$ m; $d_1 = 1.00$ m; $d_2 = 1.00$ m; $L = 15.00$ m. To the load $P = 35$ kN, $k = 2.47$ m, and is localized of $0 \leq x \leq L_1$, the fixed-end moments are $M_{BC1} = 71.4921$ kN-m and $M_{CB1} = 9.7183$ kN-m. To the load $P = 145$ kN, $k = 6.77$ m, and is found of $L_1 \leq x \leq L - L_2$, the fixed-end moments are $M_{BC2} = 376.2745$ kN-m and $M_{CB2} = 290.9268$ kN-m. To the load $P = 145$ kN, $k = 11.07$ m, and is located of $L - L_2 \leq x \leq L$, the fixed-end moments are $M_{BC3} = 102.6699$ kN-m and $M_{CB3} = 397.9590$ kN-m. The total fixed-end moments are $M_{BCT} = 550.4365$ kN-m



(a) To first and third light (A-B and C-D)



(b) To second light (B-C)

FIGURE 4. Critical position of the loads

and $M_{CBT} = 698.6041$ kN-m. The carry-over factors by Part I of this paper are obtained: $C_{BC} = 0.6441$ and $C_{CB} = 0.6441$. The stiffness factors by Part I of this paper are obtained: $k_{BC} = 7.9295$ and $k_{CB} = 7.9295$. The absolute stiffnesses are $K_{BC} = 7.9295EI/L$ and $K_{CB} = 7.9295EI/L$.

For the beam C-D: $L_1 = 4.00$ m; $L_2 = 3.00$ m; $d = 1.00$ m; $d_1 = 1.00$ m; $d_2 = 0.50$ m; $L = 12.00$ m. To the load $P = 35$ kN, $k = 0.97$ m, and is localized of $0 \leq x \leq L_1$, the fixed-end moments are $M_{CD1} = 30.7106$ kN-m and $M_{DC1} = 1.9945$ kN-m. To the load $P = 145$ kN, $k = 5.27$ m, and is found of $L_1 \leq x \leq L - L_2$, the fixed-end moments are $M_{CD2} = 344.3930$ kN-m and $M_{DC2} = 178.4415$ kN-m. To the load $P = 145$ kN, $k = 9.57$ m, and is located of $L - L_2 \leq x \leq L$, the fixed-end moments are $M_{CD3} = 73.6830$ kN-m and $M_{DC3} = 244.5827$ kN-m. The total fixed-end moments are $M_{CDT} = 448.7866$ kN-m and $M_{DCT} = 425.0187$ kN-m. The carry-over factors by Part I of this paper are obtained: $C_{CD} = 0.5348$ and $C_{DC} = 0.6968$. The stiffness factors by Part I of this paper are obtained: $k_{CD} = 8.1197$ and $k_{DC} = 6.2319$. The absolute stiffnesses are $K_{CD} = 8.1197EI/L$ and $K_{DC} = 6.2319EI/L$.

The stiffness matrix of the beam “A-B” is

$$K_{AB} = \begin{bmatrix} k_{11}^{AB} & k_{12}^{AB} \\ k_{21}^{AB} & k_{22}^{AB} \end{bmatrix} = \begin{bmatrix} 6.2319 & 4.3424 \\ 4.3424 & 8.1197 \end{bmatrix} \frac{EI_{x2}}{L}$$

where $k_{11}^{AB} = K_{AB}$; $k_{22}^{AB} = K_{BA}$; $k_{12}^{AB} = C_{AB}K_{AB}$; $k_{21}^{AB} = C_{BA}K_{BA}$; $k_{12}^{AB} = k_{21}^{AB}$.

The stiffness matrix of the beam “B-C” is

$$K_{BC} = \begin{bmatrix} k_{11}^{BC} & k_{12}^{BC} \\ k_{21}^{BC} & k_{22}^{BC} \end{bmatrix} = \begin{bmatrix} 7.9295 & 5.1074 \\ 5.1074 & 7.9295 \end{bmatrix} \frac{EI_{x2}}{L}$$

where $k_{11}^{BC} = K_{BC}$; $k_{22}^{BC} = K_{CB}$; $k_{12}^{BC} = C_{BC}K_{BC}$; $k_{21}^{BC} = C_{CB}K_{CB}$; $k_{12}^{BC} = k_{21}^{BC}$.

The stiffness matrix of the beam “C-D” is

$$K_{CD} = \begin{bmatrix} k_{11}^{CD} & k_{12}^{CD} \\ k_{21}^{CD} & k_{22}^{CD} \end{bmatrix} = \begin{bmatrix} 8.1197 & 4.3424 \\ 4.3424 & 6.2319 \end{bmatrix} \frac{EI_{x2}}{L}$$

where $k_{11}^{CD} = K_{CD}$; $k_{22}^{CD} = K_{DC}$; $k_{12}^{CD} = C_{CD}K_{CD}$; $k_{21}^{CD} = C_{DC}K_{DC}$; $k_{12}^{CD} = k_{21}^{CD}$.

General stiffness matrix “ K_G ” of the continuous beam is

$$K_G = \begin{bmatrix} k_{11}^{AB} & k_{12}^{AB} & 0 & 0 \\ k_{21}^{AB} & k_{22}^{AB} + k_{11}^{BC} & k_{12}^{BC} & 0 \\ 0 & k_{21}^{BC} & k_{22}^{BC} + k_{11}^{CD} & k_{12}^{CD} \\ 0 & 0 & k_{21}^{CD} & k_{22}^{CD} \end{bmatrix} = \begin{bmatrix} 6.2319 & 4.3424 & 0 & 0 \\ 4.3424 & 16.0492 & 5.1074 & 0 \\ 0 & 5.1074 & 16.0492 & 4.3424 \\ 0 & 0 & 4.3424 & 6.2319 \end{bmatrix} \frac{EI_{x2}}{L}$$

Fixed-end moments of the beams (phase 1) are

$$\begin{bmatrix} M_{AB} \\ M_{BA} \end{bmatrix} = \begin{bmatrix} +240.0179 \\ -556.9415 \end{bmatrix}; \quad \begin{bmatrix} M_{BC} \\ M_{CB} \end{bmatrix} = \begin{bmatrix} +550.4365 \\ -698.6041 \end{bmatrix}; \quad \begin{bmatrix} M_{CD} \\ M_{DC} \end{bmatrix} = \begin{bmatrix} +448.7866 \\ -425.0187 \end{bmatrix}$$

The vector of effective moments that act on the continuous beam is

$$\begin{bmatrix} M_A \\ M_B \\ M_C \\ M_D \end{bmatrix} = \begin{bmatrix} -240.0179 \\ +556.9415 - 550.4365 \\ +698.6041 - 448.7866 \\ +425.0187 \end{bmatrix} = \begin{bmatrix} -240.0179 \\ +6.5050 \\ +249.8175 \\ +425.0187 \end{bmatrix}$$

Force-displacement relationship is

$$[P] = [K][d]$$

where $[P]$ is the vector of effective moments that acts on the continuous beam, $[K]$ is the general stiffness matrix, and $[d]$ is the vector of displacements.

$$\begin{bmatrix} -240.0179 \\ +6.5050 \\ +249.8175 \\ +425.0187 \end{bmatrix} = \begin{bmatrix} 6.2319 & 4.3424 & 0 & 0 \\ 4.3424 & 16.0492 & 5.1074 & 0 \\ 0 & 5.1074 & 16.0492 & 4.3424 \\ 0 & 0 & 4.3424 & 6.2319 \end{bmatrix} \frac{EI_{x2}}{L} \begin{bmatrix} \beta_A \\ \beta_B \\ \beta_C \\ \beta_D \end{bmatrix}$$

The solution of the system is

$$\begin{bmatrix} \beta_A \\ \beta_B \\ \beta_C \\ \beta_D \end{bmatrix} = \begin{bmatrix} -50.64926072 \\ +17.41507643 \\ -10.38761306 \\ +75.43860956 \end{bmatrix} \frac{L}{EI_{x2}}$$

The mechanical elements associated to the analysis moments (phase 2) are

$$\begin{aligned} \begin{bmatrix} M_{AB} \\ M_{BA} \end{bmatrix} &= \begin{bmatrix} k_{11}^{AB} & k_{12}^{AB} \\ k_{21}^{AB} & k_{22}^{AB} \end{bmatrix} \begin{bmatrix} \beta_A \\ \beta_B \end{bmatrix} = \begin{bmatrix} 6.2319 & 4.3424 \\ 4.3424 & 8.1197 \end{bmatrix} \frac{EI_{x2}}{L} \begin{bmatrix} -50.64926072 \\ +17.41507643 \end{bmatrix} \frac{L}{EI_{x2}} \\ &= \begin{bmatrix} -240.0179 \\ -78.5342 \end{bmatrix} \\ \begin{bmatrix} M_{BC} \\ M_{CB} \end{bmatrix} &= \begin{bmatrix} k_{11}^{BC} & k_{12}^{BC} \\ k_{21}^{BC} & k_{22}^{BC} \end{bmatrix} \begin{bmatrix} \beta_B \\ \beta_C \end{bmatrix} = \begin{bmatrix} 7.9295 & 5.1074 \\ 5.1074 & 7.9295 \end{bmatrix} \frac{EI_{x2}}{L} \begin{bmatrix} +17.41507643 \\ -10.38761306 \end{bmatrix} \frac{L}{EI_{x2}} \\ &= \begin{bmatrix} +85.0392 \\ +6.5772 \end{bmatrix} \\ \begin{bmatrix} M_{CD} \\ M_{DC} \end{bmatrix} &= \begin{bmatrix} k_{11}^{CD} & k_{12}^{CD} \\ k_{21}^{CD} & k_{22}^{CD} \end{bmatrix} \begin{bmatrix} \beta_C \\ \beta_D \end{bmatrix} = \begin{bmatrix} 8.1197 & 4.3424 \\ 4.3424 & 6.2319 \end{bmatrix} \frac{EI_{x2}}{L} \begin{bmatrix} -10.38761306 \\ +75.43860956 \end{bmatrix} \frac{L}{EI_{x2}} \\ &= \begin{bmatrix} +243.2403 \\ +425.0187 \end{bmatrix} \end{aligned}$$

The final moments are (sum of phases 1 and 2)

$$\begin{aligned} \begin{bmatrix} M_{AB} \\ M_{BA} \end{bmatrix} &= \begin{bmatrix} +240.0179 \\ -556.9415 \end{bmatrix} + \begin{bmatrix} -240.0179 \\ -78.5342 \end{bmatrix} = \begin{bmatrix} 0 \\ -635.4757 \end{bmatrix} \\ \begin{bmatrix} M_{BC} \\ M_{CB} \end{bmatrix} &= \begin{bmatrix} +550.4365 \\ -698.6041 \end{bmatrix} + \begin{bmatrix} +85.0392 \\ +6.5772 \end{bmatrix} = \begin{bmatrix} +635.4757 \\ -692.0269 \end{bmatrix} \\ \begin{bmatrix} M_{CD} \\ M_{DC} \end{bmatrix} &= \begin{bmatrix} +448.7866 \\ -425.0187 \end{bmatrix} + \begin{bmatrix} +243.2403 \\ +425.0187 \end{bmatrix} = \begin{bmatrix} +692.0269 \\ 0 \end{bmatrix} \end{aligned}$$

Therefore, these final moments are the moments for the design of the beams.

4. Results. Tables 1 and 2 present the comparison of the proposed model against the traditional model. The proposed model (PM) considers the bending and shear deformations, and the traditional model (TM) only takes account of the bending deformations and without considering the shear deformations. Tables show the fixed-end moments factors (m_{AB} and m_{BA}) for a beam subjected to a concentrated load located anywhere on the beam. Table 1 for $L = 10d \rightarrow d = 0.10L$, $b_f = b_w + 16t_f = 0.475L$, $b_w = 0.75d = 0.075L$, $t_f = 0.25d = 0.025L$, $d_1 = d_2$, $\nu = 0.20$ of concrete. Table 2 for $L = 5d \rightarrow d = 0.20L$, $b_f = b_w + 16t_f = 0.95L$, $b_w = 0.75d = 0.15L$, $t_f = 0.25d = 0.05L$, $d_1 = d_2$, $\nu = 0.20$ of concrete. The values shown in Table 1 of the proposed model are identical to those in the tables presented in Appendix B by Tena-Colunga [7].

Another way to verify the proposed model is as follows.

1) Substituting “ $k = 0.5L$ ” and “ $L_1 = L_2 = 0L$ ” or “ $d_1 = d_2 = 0$ ” into Equations (23) and (24) of the Appendix, the fixed-end moments factors are obtained “ $m_{AB} = m_{BA} = 8$ ”. Thus, fixed-end moments are “ $M_{AB} = M_{BA} = PL/8$ ”.

2) Substituting “ $k = 0.5L$ ” and “ $L_1 = L_2 = 0L$ ” or “ $d_1 = d_2 = 0$ ” into Equations (25) and (26) of the Appendix, the fixed-end moments factors are obtained “ $m_{AB} = m_{BA} = 8$ ”. Thus, fixed-end moments are “ $M_{AB} = M_{BA} = PL/8$ ”.

3) Substituting “ $k = 0.5L$ ” and “ $L_1 = L_2 = 0L$ ” or “ $d_1 = d_2 = 0$ ” into Equations (27) and (28) of the Appendix, the fixed-end moments factors are obtained “ $m_{AB} = m_{BA} = 8$ ”. Thus, fixed-end moments are “ $M_{AB} = M_{BA} = PL/8$ ”.

4) If the fixed-end moments for the traditional model are verified with the well-known equations for uniform cross sections with a concentrated load located anywhere on the

beam ($M_{AB} = Pk(L-k)^2/L^2$ and $M_{BA} = Pk^2(L-k)/L^2$), these equations fulfill perfectly with the model presented in this paper.

One way to verify the continuity of the beam element is

1) Substituting $k = L_1$ into Equations (23) and (25) to find “ M_{AB} ”, and into Equations (24) and (26) to find “ M_{BA} ”. The results of the moments at the fixed-ends are the same.

2) Substituting $k = L - L_2$ into Equations (25) and (27) to find “ M_{AB} ”, and into Equations (26) and (28) to find “ M_{BA} ”. The results of the moments at the fixed-ends are the same.

Results for the fixed-end moment factors are as follows.

1) If the moment is greater at one support than at the opposite end, the traditional model is greater at one support, and the proposed model is greater at the opposite end.

2) The biggest differences in Table 1 are 2.2931 times the traditional model (m_{BA} , $k = 0.1L$, $L_1 = 0.1L$, $L_2 = 0.5L$, $d_2 = 2d$) and 2.1951 times the traditional model (m_{AB} , $k = 0.9L$, $L_1 = 0.3L$, $L_2 = 0.1L$, $d_2 = 2d$).

3) The biggest differences in Table 2 are 4.56 times the traditional model (m_{BA} , $k = 0.1L$, $L_1 = 0.1L$, $L_2 = 0.1L$, $d_2 = 2d$) and 4.56 times the traditional model (m_{AB} , $k = 0.9L$, $L_1 = 0.1L$, $L_2 = 0.1L$, $d_2 = 2d$).

4) Tables 1 and 2 show a relationship of TM/PM = 1.0000 in m_{AB} and m_{BA} for $k = 0.5L$ in $L_1 = 0.1L$, $L_2 = 0.1L$, $d_2/d = 0.5, 1.0, 1.5, 2.0$, also for $k = 0.5L$ in $L_1 = 0.3L$, $L_2 = 0.3L$, $d_2/d = 0.5, 1.0, 1.5, 2.0$.

Therefore, the results show that the major differences are presented in Table 2 with the parameter $d = 0.20L$.

Thus, the fixed-end moments are verified for constant or uniform cross sections.

Tables 1 and 2 show that when the beam is symmetric in load and in geometry, the fixed-end moments are the same in the traditional model and the proposed model, i.e., the shear deformations do not affect the fixed-end moments for symmetrical beams in load and in geometry.

5. Conclusions. Traditional methods used for the variable cross section members are by the Simpson’s rule to obtain the rotations or some other technique to perform numerical integration, and other authors present some tables considering the bending deformations and shear, but are limited to certain relationships and also the heights of the haunches are the same at both ends.

The main findings of this investigation are the following.

1) If the fixed-end moment factors are greater at one support than at the opposite end, the traditional model is greater at one support, and the proposed model is greater at the opposite end.

2) The fixed-end moments for symmetrical beams in load and in geometry, the fixed-end moment factors are the same for the traditional model and the proposed model, i.e., the shear deformations do not affect the fixed-end moments for symmetrical beams in load and in geometry.

3) The fixed-end moment factors are influenced by the web depth in straight haunches, i.e., if the straight haunches volume is increased, the factor is greater in the same support.

4) If the fixed-end moment factors are greater, the fixed-end moment is smaller, because the factor is located in the denominator.

5) When the parameter “ d/L ” increases, the differences are greater in the traditional model compared to the proposed model for the fixed-end moments, because the factors for the proposed model are reduced.

6) If the parameter “ d/L ” for the traditional model is modified, the fixed-end moment factors do not change their values.

7) When the concentrated load is located closer to the supports, the difference in the moments is greater between the traditional model and the proposed model.

The benefits of non-prismatic beams are as follows.

1) The T-shaped cross-sectional beams with straight haunches have been used in various structures, including buildings and bridges.

2) With the beams being tapered, the architects would be able to create and implement novel aesthetic architectural designs.

3) Structural engineers could seek for the optimum low weight-high strength systems through a redistribution of materials and beams shape.

Suggestions for future research are as follows:

1) Studying other types of non-constant cross-section;

2) Studying other types of haunches such as parabolic haunches;

3) Studying other types of loads.

REFERENCES

- [1] R. Guldán, *Frame Structures and Continuous Beams*, El Ateneo, Buenos Aires, Argentina, 1956.
- [2] *Handbook of Frame Constants: Beam Factors and Moment Coefficients for Members of Variable Section*, Portland Cement Association, 1958.
- [3] D. J. Just, Plane frameworks of tapering box and I-section, *ASCE Journal of Structural Engineering*, vol.103, no.1, pp.71-86, 1977.
- [4] H. L. Schreyer, Elementary theory for linearly tapered beams, *ASCE Journal of Structural Engineering*, vol.104, no.3, pp.515-527, 1978.
- [5] S. J. Medwadowski, Nonprismatic shear beams, *ASCE Journal of Structural Engineering*, vol.110, no.5, pp.1067-1082, 1984.
- [6] C. J. Brown, Approximate stiffness matrix for tapered beams, *ASCE Journal of Structural Engineering*, vol.110, no.12, pp.3050-3055, 1984.
- [7] A. Tena-Colunga, *Analysis of Structures with Matrix Methods*, Limusa, México, 2007.
- [8] S. B. Yuksel, Behaviour of symmetrically haunched non-prismatic members subjected to temperature changes, *Structural Engineering Mechanics*, vol.31, no.3, pp.297-314, 2009.
- [9] S. B. Yuksel, Assessment of non-prismatic beams having symmetrical parabolic haunches with constant haunch length ratio of 0.5, *Structural Engineering Mechanics*, vol.42, no.6, pp.849-866, 2012.
- [10] A. Luévanos Rojas, A mathematical model for rectangular beams of variable cross section of symmetrical parabolic shape for uniformly distributed load, *Far East Journal of Mathematical Sciences*, vol.80, no.2, pp.197-230, 2013.
- [11] A. Luévanos Rojas, A mathematical model for fixed-end moments for two types of loads for a parabolic shaped variable rectangular cross section, *Ingeniería e Investigación*, vol.34, no.2, pp.17-22, 2014.
- [12] A. Luévanos Rojas and J. Montoya Ramirez, Mathematical model for rectangular beams of variable cross section of symmetrical linear shape for uniformly distributed load, *International Journal of Innovative Computing, Information and Control*, vol.10, no.2, pp.545-564, 2014.
- [13] A. Luévanos Rojas, R. Luévanos Rojas, I. Luévanos Soto, R. G. Luévanos Vazquez and O. A. Ramirez Luévanos, Mathematical model for rectangular beams of variable cross section of symmetrical linear shape for concentrated load, *International Journal of Innovative Computing, Information and Control*, vol.10, no.3, pp.851-881, 2014.
- [14] A. Luévanos Rojas, Modeling for beams of cross section "I" subjected to a uniformly distributed load with straight haunches, *Ingeniería Mecánica Tecnología y Desarrollo*, vol.5, no.2, pp.281-292, 2015.
- [15] A. Luévanos Rojas, S. López Chavarría and M. Medina Elizondo, Modeling for mechanical elements of rectangular members with straight haunches using software: Part 1, *International Journal of Innovative Computing, Information and Control*, vol.12, no.3, pp.973-985, 2016.
- [16] A. Luévanos Rojas, S. López Chavarría and M. Medina Elizondo, Modeling for mechanical elements of rectangular members with straight haunches using software: Part 2, *International Journal of Innovative Computing, Information and Control*, vol.12, no.4, pp.1027-1041, 2016.

- [17] F. Velázquez Santillán, A. Luévanos Rojas, S. López Chavarría and M. Medina Elizondo, Modeling for beams of rectangular cross section with parabolic haunches: Part 1, *Computación y Sistemas*, vol.23, no.2, pp.557-568, 2019.
- [18] R. Sandoval Rivas, A. Luévanos Rojas, S. López Chavarría and M. Medina Elizondo, Modeling for beams of rectangular cross section with parabolic haunches: Part 2, *Computación y Sistemas*, vol.23, no.3, pp.1115-1124, 2019.
- [19] G. Balduzzi, M. Aminbaghai, E. Sacco, J. Füssl, J. Eberhardsteiner and F. Auricchio, Non-prismatic beams: A simple and effective Timoshenko-like model, *International Journal of Solids and Structures*, vol.90, pp.236-250, 2016.
- [20] I. Luévanos Soto and A. Luévanos Rojas, Modeling for fixed-end moments of I-sections with straight haunches under concentrated load, *Steel and Composite Structures*, vol.23, no.5, pp.597-610, 2017.
- [21] G. Balduzzi, S. Morganti, F. Auricchio and A. Reali, Non-prismatic Timoshenko-like beam model: Numerical solution via isogeometric collocation, *Computers and Mathematics Applications*, vol.74, no.7, pp.1531-1541, 2017.
- [22] G. Balduzzi, M. Aminbaghai, F. Auricchio and J. Füssl, Planar Timoshenko-like model for multilayer non-prismatic beams, *International Journal of Mechanics and Materials in Design*, vol.14, no.1, pp.51-70, 2018.
- [23] B. E. Montano Pérez, A. Luévanos Rojas, S. López Chavarría, M. Medina Elizondo and M. Jaramillo Rosales, Design aids for rectangular cross-section beams with straight haunches: Part 1, *International Journal of Innovative Computing, Information and Control*, vol.16, no.6, pp.1915-1928, 2020.
- [24] L. L. Gaona Tamez, A. Luévanos Rojas, S. López Chavarría, M. Medina Elizondo and M. Jaramillo Rosales, Design aids for rectangular cross-section beams with straight haunches: Part 2, *International Journal of Innovative Computing, Information and Control*, vol.16, no.6, pp.1929-1942, 2020.
- [25] C. Y. Crispin Herrera, A. Luévanos Rojas, S. López Chavarría and M. Medina Elizondo, Design aids for beams of rectangular cross section with parabolic haunches: Part 1, *Computación y Sistemas*, vol.25, no.3, pp.1-14, 2021.
- [26] R. M. Luévanos Soto, A. Luévanos Rojas, S. López Chavarría and M. Medina Elizondo, Design aids for beams of rectangular cross section with parabolic haunches: Part 2, *Computación y Sistemas*, vol.25, no.3, pp.821-834, 2021.
- [27] A. Luévanos Rojas, Method of structural analysis for statically indeterminate beams, *International Journal of Innovative Computing, Information and Control*, vol.8, no.8, pp.5473-5486, 2012.
- [28] A. Luévanos Rojas, Method of structural analysis for statically indeterminate rigid frames, *International Journal of Innovative Computing, Information and Control*, vol.9, no.5, pp.1951-1970, 2013.
- [29] A. Luévanos Rojas, Method of structural analysis, taking into account deformations by flexure, shear and axial, *International Journal of Innovative Computing, Information and Control*, vol.9, no.9, pp.3817-3838, 2013.
- [30] A. Luévanos Rojas, N. I. Kalashnykova, A. Diosdado Salazar, R. Luévanos Rojas and F. Cortés Martínez, Method of successive approximations for statically indeterminate rigid frames including a new variable, *International Journal of Innovative Computing, Information and Control*, vol.9, no.8, pp.3133-3158, 2013.
- [31] A. Luévanos Rojas, J. V. Reyes Espino and K. C. Caballero Garcia, The moment-distribution method for statically indeterminate beams using three different models, *International Journal of Innovative Computing, Information and Control*, vol.10, no.5, pp.1765-1782, 2014.
- [32] A. Luévanos Rojas and J. V. Reyes Espino, Fixed-end moments for beams subjected to a concentrated force localized anywhere taking into account the shear deformations, *International Journal of Innovative Computing, Information and Control*, vol.11, no.2, pp.463-474, 2015.
- [33] AASHTO, *AASHTO LRFD Bridge Design Specifications*, 7th Edition, American Association of State and Highway Transportation Officials, Washington, D.C., 2014.

Appendix. Fixed-end moments in support A “ M_{AB} ” and in support B “ M_{BA} ” due to a concentrated load P located from $0 \leq x \leq L_1$ are presented as follows:

$$M_{AB} = P \left[\int_0^k \left[\frac{(L-k)(L-x)x}{EI_{x1}} - \frac{(L-k)}{GA_{sx1}} \right] dx + \int_k^{L_1} \left[\frac{k(L-x)^2}{EI_{x1}} + \frac{k}{GA_{sx1}} \right] dx \right. \\ \left. + \int_{L_1}^{L-L_2} \left[\frac{k(L-x)^2}{EI_{x2}} + \frac{k}{GA_{sx2}} \right] dx \right]$$

$$\begin{aligned}
 & + \int_{L-L_2}^L \left[\frac{k(L-x)^2}{EI_{x3}} + \frac{k}{GA_{sx3}} \right] dx \left\{ \int_0^{L_1} \left[\frac{x^2}{EI_{x1}} + \frac{1}{GA_{sx1}} \right] dx \right. \\
 & + \left. \int_{L_1}^{L-L_2} \left[\frac{x^2}{EI_{x2}} + \frac{1}{GA_{sx2}} \right] dx + \int_{L-L_2}^L \left[\frac{x^2}{EI_{x3}} + \frac{1}{GA_{sx3}} \right] dx \right\} \\
 & - \left\{ \int_0^k \left[\frac{(L-k)x^2}{EI_{x1}} + \frac{(L-k)}{GA_{sx1}} \right] dx + \int_k^{L_1} \left[\frac{k(L-x)x}{EI_{x1}} - \frac{k}{GA_{sx1}} \right] dx \right. \\
 & + \left. \int_{L_1}^{L-L_2} \left[\frac{k(L-x)x}{EI_{x2}} - \frac{k}{GA_{sx2}} \right] dx \right. \\
 & + \left. \int_{L-L_2}^L \left[\frac{k(L-x)x}{EI_{x3}} - \frac{k}{GA_{sx3}} \right] dx \right\} \left\{ \int_0^{L_1} \left[\frac{(L-x)x}{EI_{x1}} - \frac{1}{GA_{sx1}} \right] dx \right. \\
 & + \left. \int_{L_1}^{L-L_2} \left[\frac{(L-x)x}{EI_{x2}} - \frac{1}{GA_{sx2}} \right] dx + \int_{L-L_2}^L \left[\frac{(L-x)x}{EI_{x3}} - \frac{1}{GA_{sx3}} \right] dx \right\} \Big/ \\
 & \left[\left\{ \int_0^{L_1} \left[\frac{(L-x)^2}{EI_{x1}} + \frac{1}{GA_{sx1}} \right] dx + \int_{L_1}^{L-L_2} \left[\frac{(L-x)^2}{EI_{x2}} + \frac{1}{GA_{sx2}} \right] dx \right. \right. \\
 & + \left. \int_{L-L_2}^L \left[\frac{(L-x)^2}{EI_{x3}} + \frac{1}{GA_{sx3}} \right] dx \right\} \left\{ \int_0^{L_1} \left[\frac{x^2}{EI_{x1}} + \frac{1}{GA_{sx1}} \right] dx \right. \\
 & + \left. \int_{L_1}^{L-L_2} \left[\frac{x^2}{EI_{x2}} + \frac{1}{GA_{sx2}} \right] dx + \int_{L-L_2}^L \left[\frac{x^2}{EI_{x3}} + \frac{1}{GA_{sx3}} \right] dx \right\} \\
 & - \left\{ \int_0^{L_1} \left[\frac{(L-x)x}{EI_{x1}} - \frac{1}{GA_{sx1}} \right] dx + \int_{L_1}^{L-L_2} \left[\frac{(L-x)x}{EI_{x2}} - \frac{1}{GA_{sx2}} \right] dx \right. \\
 & + \left. \int_{L-L_2}^L \left[\frac{(L-x)x}{EI_{x3}} - \frac{1}{GA_{sx3}} \right] dx \right\}^2 \Big] \tag{23} \\
 \\
 M_{BA} = P & \left[\left\{ \int_0^k \left[\frac{(L-k)x^2}{EI_{x1}} + \frac{(L-k)}{GA_{sx1}} \right] dx + \int_k^{L_1} \left[\frac{k(L-x)x}{EI_{x1}} - \frac{k}{GA_{sx1}} \right] dx \right. \right. \\
 & + \left. \int_{L_1}^{L-L_2} \left[\frac{k(L-x)x}{EI_{x2}} - \frac{k}{GA_{sx2}} \right] dx \right. \\
 & + \left. \int_{L-L_2}^L \left[\frac{k(L-x)x}{EI_{x3}} - \frac{k}{GA_{sx3}} \right] dx \right\} \left\{ \int_0^{L_1} \left[\frac{(L-x)^2}{EI_{x1}} + \frac{1}{GA_{sx1}} \right] dx \right. \\
 & + \left. \int_{L_1}^{L-L_2} \left[\frac{(L-x)^2}{EI_{x2}} + \frac{1}{GA_{sx2}} \right] dx + \int_{L-L_2}^L \left[\frac{(L-x)^2}{EI_{x3}} + \frac{1}{GA_{sx3}} \right] dx \right\} \\
 & - \left\{ \int_0^k \left[\frac{(L-k)(L-x)x}{EI_{x1}} - \frac{(L-k)}{GA_{sx1}} \right] dx + \int_k^{L_1} \left[\frac{k(L-x)^2}{EI_{x1}} + \frac{k}{GA_{sx1}} \right] dx \right. \\
 & + \left. \int_{L_1}^{L-L_2} \left[\frac{k(L-x)^2}{EI_{x2}} + \frac{k}{GA_{sx2}} \right] dx \right. \\
 & + \left. \int_{L-L_2}^L \left[\frac{k(L-x)^2}{EI_{x3}} + \frac{k}{GA_{sx3}} \right] dx \right\} \left\{ \int_0^{L_1} \left[\frac{(L-x)x}{EI_{x1}} - \frac{1}{GA_{sx1}} \right] dx \right. \\
 & + \left. \int_{L_1}^{L-L_2} \left[\frac{(L-x)x}{EI_{x2}} - \frac{1}{GA_{sx2}} \right] dx + \int_{L-L_2}^L \left[\frac{(L-x)x}{EI_{x3}} - \frac{1}{GA_{sx3}} \right] dx \right\} \Big/
 \end{aligned}$$

$$\begin{aligned}
& \left[\left\{ \int_0^{L_1} \left[\frac{(L-x)^2}{EI_{x1}} + \frac{1}{GA_{sx1}} \right] dx + \int_{L_1}^{L-L_2} \left[\frac{(L-x)^2}{EI_{x2}} + \frac{1}{GA_{sx2}} \right] dx \right. \right. \\
& + \left. \int_{L-L_2}^L \left[\frac{(L-x)^2}{EI_{x3}} + \frac{1}{GA_{sx3}} \right] dx \right\} \left\{ \int_0^{L_1} \left[\frac{x^2}{EI_{x1}} + \frac{1}{GA_{sx1}} \right] dx \right. \\
& + \left. \int_{L_1}^{L-L_2} \left[\frac{x^2}{EI_{x2}} + \frac{1}{GA_{sx2}} \right] dx + \int_{L-L_2}^L \left[\frac{x^2}{EI_{x3}} + \frac{1}{GA_{sx3}} \right] dx \right\} \\
& - \left\{ \int_0^{L_1} \left[\frac{(L-x)x}{EI_{x1}} - \frac{1}{GA_{sx1}} \right] dx + \int_{L_1}^{L-L_2} \left[\frac{(L-x)x}{EI_{x2}} - \frac{1}{GA_{sx2}} \right] dx \right. \\
& \left. \left. + \int_{L-L_2}^L \left[\frac{(L-x)x}{EI_{x3}} - \frac{1}{GA_{sx3}} \right] dx \right\}^2 \right] \tag{24}
\end{aligned}$$

Fixed-end moments in support A “ M_{AB} ” and in support B “ M_{BA} ” due to a concentrated load P located from $L_1 \leq x \leq L - L_2$ are presented as follows:

$$\begin{aligned}
M_{AB} = P & \left[\left\{ \int_0^{L_1} \left[\frac{(L-k)(L-x)x}{EI_{x1}} - \frac{(L-k)}{GA_{sx1}} \right] dx \right. \right. \\
& + \int_{L_1}^k \left[\frac{(L-k)(L-x)x}{EI_{x2}} - \frac{(L-k)}{GA_{sx2}} \right] dx + \int_k^{L-L_2} \left[\frac{k(L-x)^2}{EI_{x2}} + \frac{k}{GA_{sx2}} \right] dx \\
& + \int_{L-L_2}^L \left[\frac{k(L-x)^2}{EI_{x3}} + \frac{k}{GA_{sx3}} \right] dx \left\} \left\{ \int_0^{L_1} \left[\frac{x^2}{EI_{x1}} + \frac{1}{GA_{sx1}} \right] dx \right. \right. \\
& + \int_{L_1}^{L-L_2} \left[\frac{x^2}{EI_{x2}} + \frac{1}{GA_{sx2}} \right] dx + \int_{L-L_2}^L \left[\frac{x^2}{EI_{x3}} + \frac{1}{GA_{sx3}} \right] dx \left\} \right. \\
& - \left\{ \int_0^{L_1} \left[\frac{(L-k)x^2}{EI_{x1}} + \frac{(L-k)}{GA_{sx1}} \right] dx + \int_{L_1}^k \left[\frac{(L-k)x^2}{EI_{x2}} + \frac{(L-k)}{GA_{sx2}} \right] dx \right. \\
& + \int_k^{L-L_2} \left[\frac{k(L-x)x}{EI_{x2}} - \frac{k}{GA_{sx2}} \right] dx \\
& + \int_{L-L_2}^L \left[\frac{k(L-x)x}{EI_{x3}} - \frac{k}{GA_{sx3}} \right] dx \left\} \left\{ \int_0^{L_1} \left[\frac{(L-x)x}{EI_{x1}} - \frac{1}{GA_{sx1}} \right] dx \right. \right. \\
& \left. \left. + \int_{L_1}^{L-L_2} \left[\frac{(L-x)x}{EI_{x2}} - \frac{1}{GA_{sx2}} \right] dx + \int_{L-L_2}^L \left[\frac{(L-x)x}{EI_{x3}} - \frac{1}{GA_{sx3}} \right] dx \right\} \right] / \\
& \left[\left\{ \int_0^{L_1} \left[\frac{(L-x)^2}{EI_{x1}} + \frac{1}{GA_{sx1}} \right] dx + \int_{L_1}^{L-L_2} \left[\frac{(L-x)^2}{EI_{x2}} + \frac{1}{GA_{sx2}} \right] dx \right. \right. \\
& + \int_{L-L_2}^L \left[\frac{(L-x)^2}{EI_{x3}} + \frac{1}{GA_{sx3}} \right] dx \left\} \left\{ \int_0^{L_1} \left[\frac{x^2}{EI_{x1}} + \frac{1}{GA_{sx1}} \right] dx \right. \right. \\
& + \int_{L_1}^{L-L_2} \left[\frac{x^2}{EI_{x2}} + \frac{1}{GA_{sx2}} \right] dx + \int_{L-L_2}^L \left[\frac{x^2}{EI_{x3}} + \frac{1}{GA_{sx3}} \right] dx \left\} \right. \\
& - \left\{ \int_0^{L_1} \left[\frac{(L-x)x}{EI_{x1}} - \frac{1}{GA_{sx1}} \right] dx + \int_{L_1}^{L-L_2} \left[\frac{(L-x)x}{EI_{x2}} - \frac{1}{GA_{sx2}} \right] dx \right. \\
& \left. \left. + \int_{L-L_2}^L \left[\frac{(L-x)x}{EI_{x3}} - \frac{1}{GA_{sx3}} \right] dx \right\}^2 \right] \tag{25}
\end{aligned}$$

$$\begin{aligned}
 M_{BA} = P & \left[\int_0^{L_1} \left[\frac{(L-k)x^2}{EI_{x1}} + \frac{(L-k)}{GA_{sx1}} \right] dx + \int_{L_1}^k \left[\frac{(L-k)x^2}{EI_{x2}} + \frac{(L-k)}{GA_{sx2}} \right] dx \right. \\
 & + \int_k^{L-L_2} \left[\frac{k(L-x)x}{EI_{x2}} - \frac{k}{GA_{sx2}} \right] dx \\
 & + \int_{L-L_2}^L \left[\frac{k(L-x)x}{EI_{x3}} - \frac{k}{GA_{sx3}} \right] dx \left. \right\} \left\{ \int_0^{L_1} \left[\frac{(L-x)^2}{EI_{x1}} + \frac{1}{GA_{sx1}} \right] dx \right. \\
 & + \int_{L_1}^{L-L_2} \left[\frac{(L-x)^2}{EI_{x2}} + \frac{1}{GA_{sx2}} \right] dx + \int_{L-L_2}^L \left[\frac{(L-x)^2}{EI_{x3}} + \frac{1}{GA_{sx3}} \right] dx \left. \right\} \\
 & - \left\{ \int_0^{L_1} \left[\frac{(L-k)(L-x)x}{EI_{x1}} - \frac{(L-k)}{GA_{sx1}} \right] dx \right. \\
 & + \int_{L_1}^k \left[\frac{(L-k)(L-x)x}{EI_{x2}} - \frac{(L-k)}{GA_{sx2}} \right] dx + \int_k^{L-L_2} \left[\frac{k(L-x)^2}{EI_{x2}} + \frac{k}{GA_{sx2}} \right] dx \\
 & + \int_{L-L_2}^L \left[\frac{k(L-x)^2}{EI_{x3}} + \frac{k}{GA_{sx3}} \right] dx \left. \right\} \left\{ \int_0^{L_1} \left[\frac{(L-x)x}{EI_{x1}} - \frac{1}{GA_{sx1}} \right] dx \right. \\
 & + \int_{L_1}^{L-L_2} \left[\frac{(L-x)x}{EI_{x2}} - \frac{1}{GA_{sx2}} \right] dx + \int_{L-L_2}^L \left[\frac{(L-x)x}{EI_{x3}} - \frac{1}{GA_{sx3}} \right] dx \left. \right\} / \\
 & \left[\left\{ \int_0^{L_1} \left[\frac{(L-x)^2}{EI_{x1}} + \frac{1}{GA_{sx1}} \right] dx + \int_{L_1}^{L-L_2} \left[\frac{(L-x)^2}{EI_{x2}} + \frac{1}{GA_{sx2}} \right] dx \right. \right. \\
 & + \left. \int_{L-L_2}^L \left[\frac{(L-x)^2}{EI_{x3}} + \frac{1}{GA_{sx3}} \right] dx \right\} \left\{ \int_0^{L_1} \left[\frac{x^2}{EI_{x1}} + \frac{1}{GA_{sx1}} \right] dx \right. \\
 & + \left. \int_{L_1}^{L-L_2} \left[\frac{x^2}{EI_{x2}} + \frac{1}{GA_{sx2}} \right] dx + \int_{L-L_2}^L \left[\frac{x^2}{EI_{x3}} + \frac{1}{GA_{sx3}} \right] dx \right\} \\
 & - \left\{ \int_0^{L_1} \left[\frac{(L-x)x}{EI_{x1}} - \frac{1}{GA_{sx1}} \right] dx + \int_{L_1}^{L-L_2} \left[\frac{(L-x)x}{EI_{x2}} - \frac{1}{GA_{sx2}} \right] dx \right. \\
 & \left. + \int_{L-L_2}^L \left[\frac{(L-x)x}{EI_{x3}} - \frac{1}{GA_{sx3}} \right] dx \right\}^2 \quad (26)
 \end{aligned}$$

Fixed-end moments in support A “ M_{AB} ” and in support B “ M_{BA} ” due to a concentrated load P located from $L - L_2 \leq x \leq L$ are presented as follows:

$$\begin{aligned}
 M_{AB} = P & \left[\int_0^{L_1} \left[\frac{(L-k)(L-x)x}{EI_{x1}} - \frac{(L-k)}{GA_{sx1}} \right] dx \right. \\
 & + \int_{L_1}^{L-L_2} \left[\frac{(L-k)(L-x)x}{EI_{x2}} - \frac{(L-k)}{GA_{sx2}} \right] dx \\
 & + \int_{L-L_2}^k \left[\frac{(L-k)(L-x)x}{EI_{x3}} - \frac{(L-k)}{GA_{sx3}} \right] dx \\
 & + \int_k^L \left[\frac{k(L-x)^2}{EI_{x3}} + \frac{k}{GA_{sx3}} \right] dx \left. \right\} \left\{ \int_0^{L_1} \left[\frac{x^2}{EI_{x1}} + \frac{1}{GA_{sx1}} \right] dx \right. \\
 & + \left. \int_{L_1}^{L-L_2} \left[\frac{x^2}{EI_{x2}} + \frac{1}{GA_{sx2}} \right] dx + \int_{L-L_2}^L \left[\frac{x^2}{EI_{x3}} + \frac{1}{GA_{sx3}} \right] dx \right\}
 \end{aligned}$$

$$\begin{aligned}
& - \left\{ \int_0^{L_1} \left[\frac{(L-k)x^2}{EI_{x1}} + \frac{(L-k)}{GA_{sx1}} \right] dx + \int_{L_1}^{L-L_2} \left[\frac{(L-k)x^2}{EI_{x2}} + \frac{(L-k)}{GA_{sx2}} \right] dx \right. \\
& + \int_{L-L_2}^k \left[\frac{(L-k)x^2}{EI_{x3}} + \frac{(L-k)}{GA_{sx3}} \right] dx \\
& + \int_k^L \left[\frac{k(L-x)x}{EI_{x3}} - \frac{k}{GA_{sx3}} \right] dx \left. \right\} \left\{ \int_0^{L_1} \left[\frac{(L-x)x}{EI_{x1}} - \frac{1}{GA_{sx1}} \right] dx \right. \\
& + \int_{L_1}^{L-L_2} \left[\frac{(L-x)x}{EI_{x2}} - \frac{1}{GA_{sx2}} \right] dx + \int_{L-L_2}^L \left[\frac{(L-x)x}{EI_{x3}} - \frac{1}{GA_{sx3}} \right] dx \left. \right\} / \\
& \left[\left\{ \int_0^{L_1} \left[\frac{(L-x)^2}{EI_{x1}} + \frac{1}{GA_{sx1}} \right] dx + \int_{L_1}^{L-L_2} \left[\frac{(L-x)^2}{EI_{x2}} + \frac{1}{GA_{sx2}} \right] dx \right. \right. \\
& + \left. \int_{L-L_2}^L \left[\frac{(L-x)^2}{EI_{x3}} + \frac{1}{GA_{sx3}} \right] dx \right\} \left\{ \int_0^{L_1} \left[\frac{x^2}{EI_{x1}} + \frac{1}{GA_{sx1}} \right] dx \right. \\
& + \left. \int_{L_1}^{L-L_2} \left[\frac{x^2}{EI_{x2}} + \frac{1}{GA_{sx2}} \right] dx + \int_{L-L_2}^L \left[\frac{x^2}{EI_{x3}} + \frac{1}{GA_{sx3}} \right] dx \right\} \\
& - \left\{ \int_0^{L_1} \left[\frac{(L-x)x}{EI_{x1}} - \frac{1}{GA_{sx1}} \right] dx + \int_{L_1}^{L-L_2} \left[\frac{(L-x)x}{EI_{x2}} - \frac{1}{GA_{sx2}} \right] dx \right. \\
& + \left. \int_{L-L_2}^L \left[\frac{(L-x)x}{EI_{x3}} - \frac{1}{GA_{sx3}} \right] dx \right\}^2 \tag{27} \\
M_{BA} = P & \left[\left\{ \int_0^{L_1} \left[\frac{(L-k)x^2}{EI_{x1}} + \frac{(L-k)}{GA_{sx1}} \right] dx + \int_{L_1}^{L-L_2} \left[\frac{(L-k)x^2}{EI_{x2}} + \frac{(L-k)}{GA_{sx2}} \right] dx \right. \right. \\
& + \int_{L-L_2}^k \left[\frac{(L-k)x^2}{EI_{x3}} + \frac{(L-k)}{GA_{sx3}} \right] dx \\
& + \int_k^L \left[\frac{k(L-x)x}{EI_{x3}} - \frac{k}{GA_{sx3}} \right] dx \left. \right\} \left\{ \int_0^{L_1} \left[\frac{(L-x)^2}{EI_{x1}} + \frac{1}{GA_{sx1}} \right] dx \right. \\
& + \int_{L_1}^{L-L_2} \left[\frac{(L-x)^2}{EI_{x2}} + \frac{1}{GA_{sx2}} \right] dx + \int_{L-L_2}^L \left[\frac{(L-x)^2}{EI_{x3}} + \frac{1}{GA_{sx3}} \right] dx \left. \right\} \\
& - \left\{ \int_0^{L_1} \left[\frac{(L-k)(L-x)x}{EI_{x1}} - \frac{(L-k)}{GA_{sx1}} \right] dx \right. \\
& + \int_{L_1}^{L-L_2} \left[\frac{(L-k)(L-x)x}{EI_{x2}} - \frac{(L-k)}{GA_{sx2}} \right] dx \\
& + \int_{L-L_2}^k \left[\frac{(L-k)(L-x)x}{EI_{x3}} - \frac{(L-k)}{GA_{sx3}} \right] dx \\
& + \int_k^L \left[\frac{k(L-x)^2}{EI_{x3}} + \frac{k}{GA_{sx3}} \right] dx \left. \right\} \left\{ \int_0^{L_1} \left[\frac{(L-x)x}{EI_{x1}} - \frac{1}{GA_{sx1}} \right] dx \right. \\
& + \int_{L_1}^{L-L_2} \left[\frac{(L-x)x}{EI_{x2}} - \frac{1}{GA_{sx2}} \right] dx + \int_{L-L_2}^L \left[\frac{(L-x)x}{EI_{x3}} - \frac{1}{GA_{sx3}} \right] dx \left. \right\} / \\
& \left[\left\{ \int_0^{L_1} \left[\frac{(L-x)^2}{EI_{x1}} + \frac{1}{GA_{sx1}} \right] dx + \int_{L_1}^{L-L_2} \left[\frac{(L-x)^2}{EI_{x2}} + \frac{1}{GA_{sx2}} \right] dx \right. \right.
\end{aligned}$$

$$\begin{aligned}
& + \int_{L-L_2}^L \left[\frac{(L-x)^2}{EI_{x3}} + \frac{1}{GA_{sx3}} \right] dx \left\{ \int_0^{L_1} \left[\frac{x^2}{EI_{x1}} + \frac{1}{GA_{sx1}} \right] dx \right. \\
& + \int_{L_1}^{L-L_2} \left[\frac{x^2}{EI_{x2}} + \frac{1}{GA_{sx2}} \right] dx + \int_{L-L_2}^L \left[\frac{x^2}{EI_{x3}} + \frac{1}{GA_{sx3}} \right] dx \left. \right\} \\
& - \left\{ \int_0^{L_1} \left[\frac{(L-x)x}{EI_{x1}} - \frac{1}{GA_{sx1}} \right] dx + \int_{L_1}^{L-L_2} \left[\frac{(L-x)x}{EI_{x2}} - \frac{1}{GA_{sx2}} \right] dx \right. \\
& \left. + \int_{L-L_2}^L \left[\frac{(L-x)x}{EI_{x3}} - \frac{1}{GA_{sx3}} \right] dx \right\}^2 \tag{28}
\end{aligned}$$

Author Biography



Omar Sierra-Andrade received the Master's degree in Management and Strategic Planning from the Universidad Autónoma de San Luis Potosí (2016) and the degree of Doctor in Administration and Senior Management (2023) from the Facultad de Contaduría y Administración of the Universidad Autónoma de Coahuila. He is Deputy Regional Sales Director at Compartamos Banco since 2008 in Torreón, Coahuila. He has experience in national and international passenger transportation, creating a company in the United States of America, to offer an international passenger service according with the Federal Motor Carrier Safety Administration. He is professor and researcher of the Facultad de Contaduría y Administración, Torreón Campus of the Universidad Autónoma de Coahuila. His research interests are mathematical models applied to Finance and Administration.



Arnulfo Luévanos-Rojas received his B.Sc. degree in Civil Engineering (1981), Master in Science with Specialization in Structures (1983), Master in Science with Specialization in Planning and Construction of Works (2000), Master in Administration (2004), and Doctor in Engineering with Specialization in Planning Systems and Construction (2009). He was professor and researcher of the Facultad de Ingeniería, Ciencias y Arquitectura, Gomez Palacio Campus of the Universidad Juárez del Estado de Durango from 2006 to 2015, and of the Facultad de Contaduría y Administración, Torreón Campus of the Universidad Autónoma de Coahuila since 2015 to date. He has published more than 122 papers in journals indexed in the Web of Science. His research interests are mathematical models applied to Engineering and Administration. He is member of the National System of Researchers of Mexico (Level I from 2016-2022 and Level II from 2023-2027). He is an Honorary State Researcher for the State of Coahuila, Mexico. He has received several distinctions: Distinguished Professor by ULSA (Universidad La Salle Laguna) 2002, 2007, 2010; Researcher of the year 2023 by UAC (Universidad Autónoma de Coahuila); He has been included in the "2023 World's Top 2% Scientists List" by Stanford University.



Blanca Estela Montano-Pérez received the Master's degree in Education, Specialty in Child Psychology, Bachelor in Psychology (2015) and the degree of Doctor in Administration and Senior Management (2019) from the Facultad de Contaduría y Administración of the Universidad Autónoma de Coahuila. She is professor and researcher of the Facultad de Contaduría y Administración, Monclova Campus of the Universidad Autónoma de Coahuila. Her research interests are mathematical models applied to Administration. She is member of the National System of Researchers of Mexico (Level I from 2023-2027). She is an Honorary State Researcher for the State of Coahuila, Mexico.